United States
Environmental Protection
Agency

Industrial Environmental Research
Laboratory
Research Triangle Park NC 27711

EPA-600/7-80-077
April 1980

EPA

Charge Measurements of Particles Exiting Electrostatic Precipitators

Interagency Energy/Environment R&D Program Report

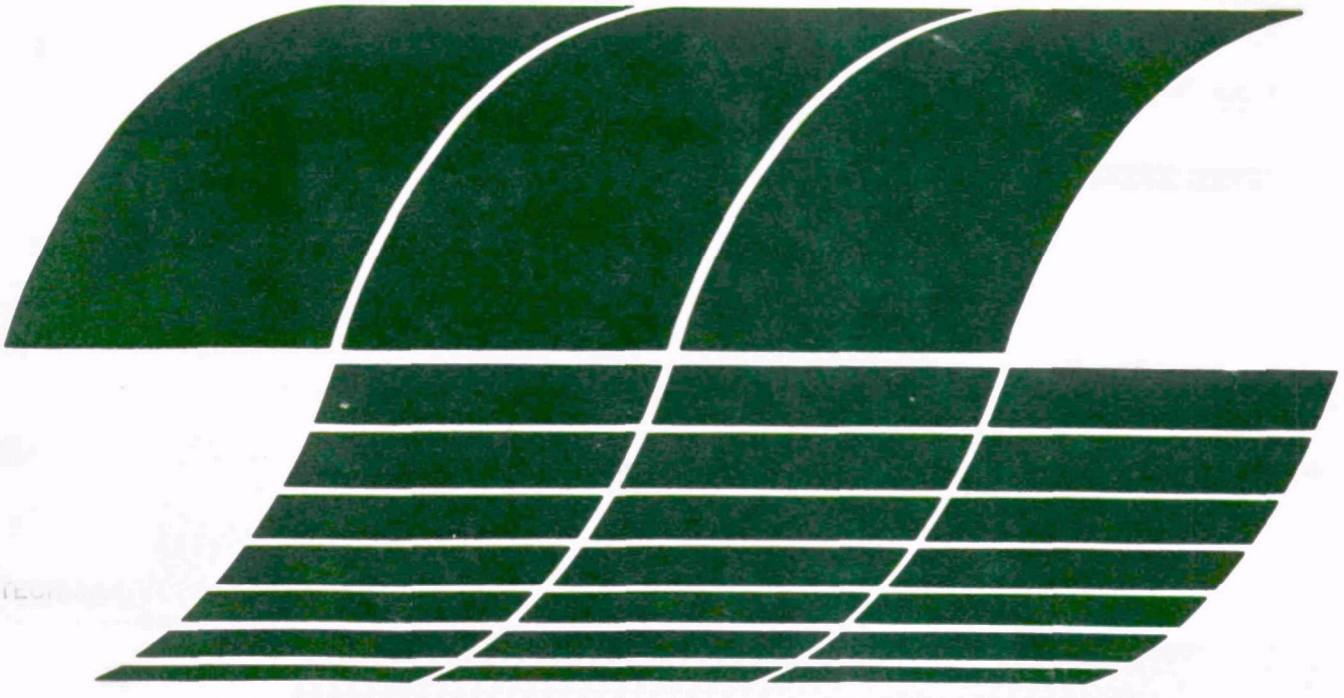

RESEARCH REPORTING SERIES

Research reports of the Office of Research and Development, U.S. Environmental Protection Agency, have been grouped into nine series. These nine broad categories were established to facilitate further development and application of environmental technology. Elimination of traditional grouping was consciously planned to foster technology transfer and a maximum interface in related fields. The nine series are:

1. Environmental Health Effects Research
2. Environmental Protection Technology
3. Ecological Research
4. Environmental Monitoring
5. Socioeconomic Environmental Studies
6. Scientific and Technical Assessment Reports (STAR)
7. Interagency Energy-Environment Research and Development
8. "Special" Reports
9. Miscellaneous Reports

This report has been assigned to the INTERAGENCY ENERGY-ENVIRONMENT RESEARCH AND DEVELOPMENT series. Reports in this series result from the effort funded under the 17-agency Federal Energy/Environment Research and Development Program. These studies relate to EPA's mission to protect the public health and welfare from adverse effects of pollutants associated with energy systems. The goal of the Program is to assure the rapid development of domestic energy supplies in an environmentally-compatible manner by providing the necessary environmental data and control technology. Investigations include analyses of the transport of energy-related pollutants and their health and ecological effects; assessments of, and development of, control technologies for energy systems; and integrated assessments of a wide range of energy-related environmental issues.

EPA REVIEW NOTICE

This report has been reviewed by the participating Federal Agencies, and approved for publication. Approval does not signify that the contents necessarily reflect the views and policies of the Government, nor does mention of trade names or commercial products constitute endorsement or recommendation for use.

This document is available to the public through the National Technical Information Service, Springfield, Virginia 22161.

EPA-600/7-80-077

April 1980

Charge Measurements of Particles Exiting Electrostatic Precipitators

by

J.R. McDonald, M.H. Anderson, and R.B. Mosley

Southern Research Institute
2000 Ninth Avenue, South
Birmingham, Alabama 35205

Contract No. 68-02-2610
Program Element No. EHE624

EPA Project Officer: Leslie E. Sparks

Industrial Environmental Research Laboratory
Office of Environmental Engineering and Technology
Research Triangle Park, NC 27711

Prepared for

U.S. ENVIRONMENTAL PROTECTION AGENCY
Office of Research and Development
Washington, DC 20460

ABSTRACT

The objective of this research was to investigate particle charging in positive and negative corona discharge as a function of temperature from 38°C to 343°C in order to establish, especially at hot-side precipitator temperatures, the relative effectiveness of the two possible methods of charging.

In positive corona discharge, only positive ions can participate in the particle charging process. In negative corona discharge, there is the potential for both negative ions and free electrons to participate in the particle charging process. Thus, since different charging mechanisms are possible for positive and negative corona discharge, the values of particle charge obtained under similar electrical operating conditions for the two cases might differ.

The values of charge on individual particles exiting two different laboratory precipitators have been measured in an experimental apparatus which utilizes a Millikan cell. The measurement system was capable of obtaining data on particles with radii down to approximately 0.2 μm. Measurements were directed at fine particles with radii approximately between 0.3 μm and 1.5 μm. Measurements were obtained for redispersed fly ash particles carried in air at temperatures from 38°C to 343°C. The electrode geometries and electrical operating conditions utilized in the experiments are typical of full-scale precipitators.

At comparable voltages and currents for positive and negative corona discharges, the data show that the ratio of the values of negative to positive charge for radii in the range 0.6-1.3 μm increases from a value of approximately 1 to a value of approximately 2 as the temperature increases from 37°C to 343°C. The predictions of a mathematical model of electrostatic precipitation which employs an ionic charging theory show good agreement with all the positive charging data, but show good agreement with the negative charging data only at temperatures below 37°C. The differences in the measurements and the model predictions are consistent with the postulation of free electron charging at elevated temperatures in negative corona discharge.

This report is submitted in partial fulfillment of Contract 68-02-2610, Task 10, by Southern Research Institute under sponsorship of the U.S. Environmental Protection Agency. This report covers the period October 1, 1978, to March 10, 1979, when it was completed.

CONTENTS

FIGURES

TABLES

ACKNOWLEDGMENTS

Precipitator C referred to in this report was provided for use during this project by the U.S. Environmental Protection Agency, Industrial Environmental Research Laboratory, Particulate Technology Branch (PATB). The authors would like to thank EPA personnel, G. Ramsey, B. Daniel, R. Valentine, and R. Ogan, for their assistance.

NOMENCLATURE

F_D	net downward force, nt
m	mass of the particle, kg
a_D	downward acceleration, m/sec^2
q	charge on the particle, coul
E	electric field, V/m
g	acceleration due to gravity, m/sec^2
F_d	drag force acting on the particle, nt
ρ_p	density of the particle, kg/m^3
ρ_a	density of the gaseous medium, kg/m^3
a	particle radius, m
η	viscosity of the gaseous medium, $nt\text{-}sec/m^2$
V_D	downward velocity of the particle, m/sec
$(1+A\ell/a)$	Cunningham correction factor,
ℓ	molecular mean free path, m
$A = 1.257 + 0.400 \exp(-1.10\ a/\ell)$	
F_u	net upward force, nt
a_u	upward acceleration, m/sec^2
v_u	upward velocity of the particle, m/sec
S	distance over which the particle moves, m
t_D	time to fall the distance S, sec
t_u	time to rise the distance S, sec
E	V/D electric field between two parallel plates, V/m
V	voltage applied across two parallel plates, V
D	spacing between the parallel plates, m

METRIC CONVERSION FACTORS

To convert from	To	Multiply by
ft	m	0.3048
in.	cm	2.54
$\mu A/ft^2$	nA/cm^2	1.075
ft/sec	m/sec	0.3048
gr/acf	gm/m^3	2.28

To convert from °F to °C: $°C = \frac{°F + 459}{1.8} - 273.3$

SECTION 1

INTRODUCTION

In the electrostatic precipitation process, particles suspended in a moving gas stream are charged as the gas is passed through a corona discharge. The particles are charged due to collisions with molecular ions and, possibly, free (unattached) electrons in the case of negative corona discharge. Since the force which drives a charged particle to a collection electrode is proportional to the charge on the particle, the mechanisms involved in the particle charging process and the attainable values of particle charge under various operating conditions are of fundamental importance with respect to understanding and utilizing the electrostatic precipitation process.

In the positive corona discharge, the electrons created in the avalanche process near the discharge electrode migrate to the discharge electrode leaving behind positive molecular ions which migrate through the interelectrode space toward the collection electrode. In this case, the interelectrode space, exclusive of the relatively small region near the discharge electrode where active gas breakdown occurs, consists of neutral gas molecules and positive molecular ions. Therefore, for the positive corona case, only positive ions can participate in the particle charging process.

Evidence and conjecture of the presence of free electron charging has been documented in the literature for laboratory charging experiments with small-scale charging devices at room temperature.[1,2] The mechanism by which free electrons charge particles could be quite different than that for ionic charging. Intuitively, the extent of free electron charging should depend on the electrode geometry (especially the spacing between the discharge and collection electrodes), applied voltage, gas temperature, and gas pressure. At the present, the mechanisms by which electrons would charge particles have not been described theoretically, and no experimental data are available that truly isolate electron charging from ionic charging. In applying fundamental principles to full-scale precipitators, effects due to free electrons are generally neglected.

The purpose of the work presented here was to make charge and radius measurements on individual fly ash particles in a typical full-scale, electrode geometry at various temperatures up to that which is typical in a hot-side precipitator. The values of charge and radius of individual particles exiting two different laboratory precipitators have been measured with an experimental apparatus which utilizes a Millikan cell. Measurements were obtained for redispersed fly ash particles at temperatures from 38 to 343°C at various voltages and current densities typical of full-scale precipitator operating conditions.

It was anticipated that by making the above measurements two questions of importance could be answered. The first question relates to how positive and negative coronas compare in effectiveness for charging particles. Higher voltages and currents before sparkover may result with one type of corona discharge and may lead to significantly higher values of particle charge. The possibly different charging mechanisms in the cases of positive and negative coronas may result in significantly different values of particle charge under similar operating conditions. The second question relates to whether free electrons in the case of negative corona significantly enhance particle charging at higher temperatures (and/or reduced pressures). Recent field data from a hot-side precipitator collecting fly ash indicate enhanced collection efficiencies for particles with radii between 0.5 and 1.5 μm^3. These collection efficiencies were predicted by using the measured operating voltages and current densities in conjunction with an ionic charging theory and were significantly lower than those measured. In this case, free electron charging may have been prominent in the electrostatic precipitation process.

SECTION 2

SUMMARY AND CONCLUSIONS

The apparatus and technique described for measuring particle radius and charge are capable of providing reliable data on individual particles charged in an electrostatic precipitation device. For temperatures up to 343°C (650°F), the measured values of charge acquired in positive corona by particles with radii in the range between 0.3 μm and 1.5 μm are in good agreement with those predicted by an ionic charging theory. For temperatures less than 37°C (100°F), the measured values of charge acquired in negative corona by particles with radii in the range between 0.3 μm and 1.5 μm are in good agreement with those predicted by an ionic charging theory. For temperatures of 232°C (450°F) and 343°C (650°F), the measured values of charge acquired in negative corona by particles with radii between 0.6 μm and 1.3 μm are significantly higher than those measured for positive corona under similar conditions and those predicted from a completely ionic charging theory. These data indicate that the charging mechanisms for positive and negative corona differ as temperature increases. The enhanced values of particle charge for negative corona at elevated temperatures are consistent with the postulation of a free electron contribution in the particle charging mechanism. Thus, a general theory for particle charging in negative corona must contain ionic and electronic charging mechanisms whose relative contributions are temperature dependent. The data indicate that, even in a full-scale precipitator utilizing negative corona, the effect of free electrons on the charging process can not be ignored for typical temperatures between 148°C (300°F) and 371°C (700°F).

SECTION 3

RECOMMENDATIONS

Since the results of this work indicate that at temperatures greater than 148°C (300°F) particle charging in full-scale electrode geometries with negative corona is more effective than with positive corona and that the values of particle charge obtained in negative corona at these temperatures can not be predicted by an ionic charging theory, it is recommended that further work be done to better describe these results. Since possible free electron charging in negative corona offers the only significant physical difference between positive and negative corona, it is recommended that particle charging due to free electrons be investigated in the future. Presently, no data are available that truly isolate free electron charging from ionic charging. Therefore, it is recommended that experiments be designed and performed to study isolated free electron charging of particles as a function of electron density, particle residence time, electric field strength, particle diameter, gas pressure, and gas temperature. Also, since there is no adequate free electron charging theory presently available, it is recommended that work be performed to develop such a theory.

SECTION 4

MEASUPEMENT TECHNIQUE AND APPARATUS

The technique utilized for simultaneously determining the charge and radius of a particle is based on the downward and upward motion of a charged particle in an insulating gas under the influence of a uniform, reversible electric field. When the gravitational force and the force due to the electric field act on the charged particle in the same direction, then the charged particle will experience a net downward force given by

$$F_D = ma_D = -qE - mg + F_d$$
$$= -qE - (\rho_p - \rho_a)(\tfrac{4}{3}\pi a^3)g + (6\pi\eta a v_D)/(1 + A\ell/a), \quad (1)$$

where

F_D = net downward force (nt),

m = mass of the particle (kg),

a_D = downward acceleration (m/sec^2),

q = charge on the particle (coul),

E = electric field (V/m),

g = acceleration due to gravity (m/sec^2),

F_d = drag force acting on the particle (nt),

ρ_p = density of the particle (kg/m^3),

ρ_a = density of the gaseous medium (kg/m^3),

a = particle radius (m),

η = viscosity of the gaseous medium ($nt\text{-}sec/m^2$),

v_D = downward velocity of the particle (m/sec),

$(1+A\ell/a)$ = Cunningham correction factor,

ℓ = molecular mean free path, (m), and

$A = 1.257 + 0.400 \exp(-1.10\ a/\ell)$.

Similarly, the force acting on the charged particle due to the electric field can be made opposite to that of the gravitational force in such a manner that the charged particle will experience a net upward force given by

$$F_u = ma_u = qE - mg - F_d$$
$$= qE - (\rho_p - \rho_a)(\tfrac{4}{3}\pi a^3)g - (6\pi\eta v_u)/(1 + A\ell/a), \quad (2)$$

where

F_u = net upward force (nt),

a_u = upward acceleration (m/sec^2),

v_u = upward velocity of the particle (m/sec),

and all other symbols are as previously defined.

Assuming that the terminal velocity of the particle is reached instantaneously, then $a_u = a_D = 0$ and

$$v_D = S/t_D \quad (3)$$

and

$$v_u = S/t_u, \quad (4)$$

where

S = distance over which the particle moves (m),

t_D = time to fall the distance S (sec), and

t_u = time to rise the distance S (sec).

Adding equations (1) and (2) yields

$$-(\tfrac{8}{3}\pi a^3)(\rho_p - \rho_a)g + [(6\pi\eta aS)/(1 + A\ell/a)]\ (\frac{1}{t_D} - \frac{1}{t_u}) = 0. \quad (5)$$

Subtracting equations (1) and (2) yields

$$- 2\,qE + [(6\pi\eta aS)/(1 + A\ell/a)]\,\left(\frac{1}{t_D} + \frac{1}{t_u}\right) = 0. \qquad (6)$$

Equations (5) and (6) can be solved simultaneously to obtain expressions for a and q.

Equation (5) can be rewritten in the form

$$a^2 + (A\ell)a + \frac{9\eta S}{4(\rho_p - \rho_a)\,g}\left(\frac{1}{t_u} - \frac{1}{t_D}\right) = 0. \qquad (7)$$

Solving for a yields

$$a = \frac{-A\ell + \sqrt{A^2\ell^2 - \frac{9\eta S}{(\rho_p - \rho_a)\,g}\left(\frac{1}{t_u} - \frac{1}{t_D}\right)}}{2}. \qquad (8)$$

Solving equation (6) for q yields

$$q = \frac{D}{V}\,[(3\pi\eta aS)/(1 + A\ell/a)]\,\left(\frac{1}{t_D} + \frac{1}{t_u}\right), \qquad (9)$$

where

E = V/D,

V = voltage applied across two parallel plates (V), and

D = spacing between the parallel plates (m).

A technique and apparatus have been developed for measuring the radius and charge on individual particles which have been treated in an electrostatic precipitation device. The technique consists of extracting a sample of gas from the precipitation device and directing part of this extracted sample into a modified Millikan measurement cell. A single particle can then be isolated, and its transit times in a uniform electric field can be utilized in equations (8) and (9) to determine its radius and charge.

A drawing of the measurement apparatus with its insertion into a precipitator is shown in Figure 1. The gas sample is extracted through two-inch diameter tubing. At temperatures less than 204°C, the tubing can be made of teflon or metal with equivalent results. This tubing contains two bends and is electrically grounded through a spiral wire which runs along the inner surface of the tubing. The tubing runs upward from the measurement cell

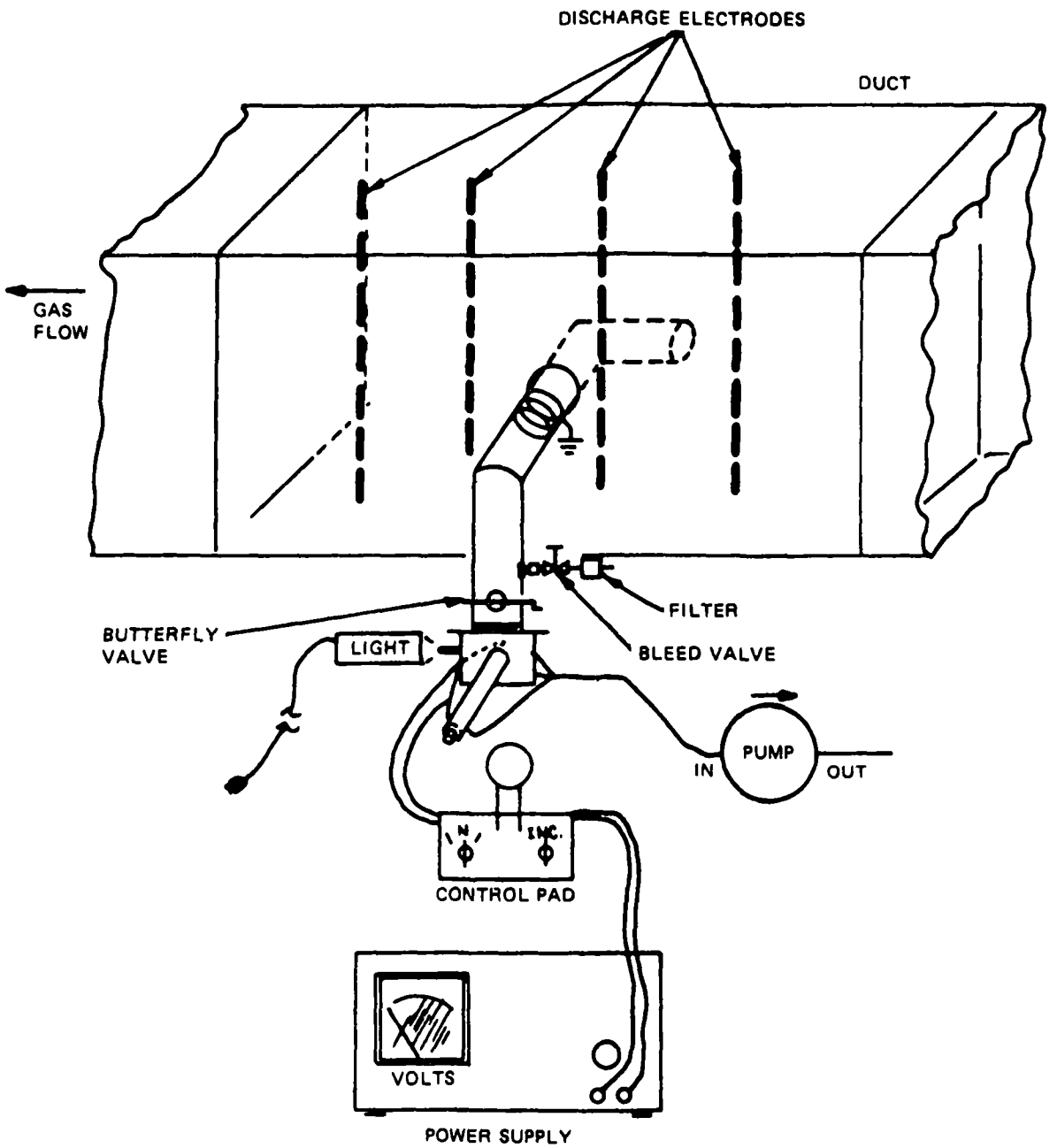

Figure 1. Experimental apparatus for measuring the radius and charge of particles.

and makes a right angle bend so that the tubing can enter a sampling port. The second bend in the tubing is made so that the tubing will be antiparallel to the gas flow and so that the entrance to the tubing can be located inside the electrified regions although the port is located downstream from these regions. The tubing leading down to the measurement cell contains a butterfly valve which can be opened to allow a sample to be drawn into the measurement cell and can be closed to prevent the gas sample from being drawn back into a precipitation device which has negative pressure inside and to prevent air flow disturbances during the measurements. Below this valve and below the measurement cell there is a connection to a pump. With the valve open, the pump is operated and particles are drawn into the measurement cell. When a sufficient number of particles is obtained in the measurement cell, the pump is turned off with simultaneous closing of the valve. Once the pump is turned off and the valve is closed, the particles very quickly cease to have any motion due to gas flow. At this point, only the gravitational field, viscous drag, and electric field which can be imposed across the parallel plates of the measurement cell have any influence on the motion of the particles.

In those cases where the particle concentrations are too large for easy isolation of individual particles, the extracted gas sample can be diluted. Filtered, outside air can be mixed with the extracted sample by means of a bleed valve preceded by a filter.

The Millikan measurement cell is cylindrical in shape with a diameter of 3.8 cm and a plate spacing (or approximate height) of 0.5 cm. Gas enters the cell through a small hole in a conical depression in the top plate. The particles are illuminated by a high intensity microscope lamp and are viewed through a microscope attached to the measurement cell. The distance traveled by the particles is determined by a graticule which is mounted near the focal plane of the objective lens of the microscope. Measurement of the particle transit times was performed with a stopwatch. Voltages on the order of 3 to 15 volts were applied across the plates to produce the electric fields necessary to generate the data presented in this report. The temperature of the gas in the measurement cell was determined by means of a thermocouple.

In the system described here, particles with radii down to approximately 0.2 μm can be observed. Measurements were concerned primarily with fine particles with diameters approximately between 0.3 μm and 1.5 μm since (1) they are the most difficult to collect in a precipitator, (2) their behavior in a precipitator is the most difficult to model, and (3) their escape into the atmosphere offers the greatest health hazard. Measurements on smaller particles can be readily obtained by allowing the larger

particles to settle out. By waiting approximately three minutes after a new sample is introduced into the measurement cell, only particles of approximately 0.5 μm or less in radius will remain in the field of view. Measurements on the larger particles can be readily made by choosing those particles which fall the fastest under the influence of gravity. The measurement system also has the capability of determining the magnitude and sign of the charge on a particle. Thus, the system has the potential to be used to analyze the effects on particle charge of back corona and rapping reentrainment. In addition, particles can be successfully extracted and analyzed from electrified regions at different locations in a precipitation device.

SECTION 5

EXPERIMENTAL PROGRAM, DATA, AND RESULTS

The capability of the technique and apparatus to make accurate measurements of the radius and charge of particles treated in an electrostatic precipitator has been demonstrated in previous work. Measurements were performed under essentially idealized conditions in laboratory Precipitator A. This precipitator has one gas passage, four electrical sections which are 0.76 m (2.5 ft) long, plates which are 38.1 cm (15 in.) high, a 25.4 cm (10 in.) plate-to-plate spacing, a 12.7 cm (5 in.) wire-to-wire spacing, and a 0.24 cm (0.094 in.) discharge electrode (wire) diameter. The normalized standard deviation of the gas velosity distribution and the gas sneakage per baffled electrical section were both measured to be less than 10%. For the experiments in laboratory Precipitator A, low mass concentrations of dioctylphthalate (DOP) droplets were generated by an aerosol sprayer and were carried through the precipitator by air at ambient conditions. Since (1) the particles were spherical, (2) particle reentrainment could not exist, and (4) gas sneakage was minimal, the results of the measurements could be interpreted with little ambiguity.

Measurements were made at precipitator operating conditions consisting of negative corona, an average applied voltage of 44.2 kV, an average current density of 21.5 nA/cm^2 (20.0 $\mu A/ft^2$), and a gas velocity of 1.5 m/sec (4.9 ft/sec). The data obtained at the precipitator outlet from the measurements on 486 individual particles are shown graphically in Figure 2 and are tabulated in Table 1. The data on each individual particle were obtained from the average values of three measurements each of the time required for the particle to travel downward a distance of 0.129 cm under the influence of an electric field and of the time required to travel the same distance upward. The bars on the average data points are one standard deviation and are not necessarily representative of the error in the measurement technique but, instead, they are more representative of the expected spread in charge on a particle with a given radius due to the fact that different particles travel different paths through the precipitator and experience different charging electric field strengths and ion densities. Also, particle radii in a narrow band have been grouped together with a radius given by the midpoint of the band.

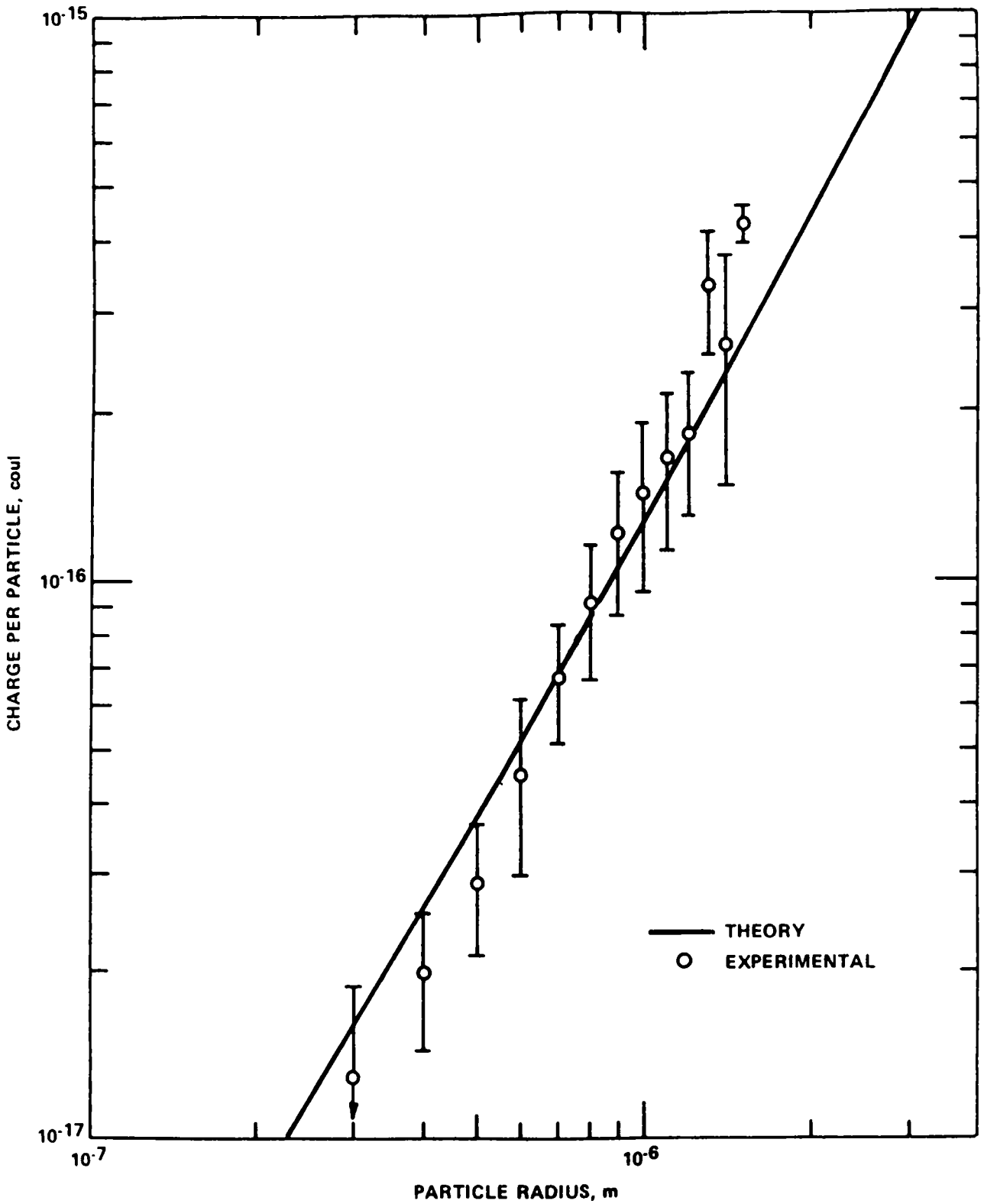

Figure 2. Theoretical and measured particle charge as a function of particle radius at the outlet of laboratory Precipitator A at ambient temperature.

TABLE 1. MEASURED AND PREDICTED VALUES OF PARTICLE CHARGE AT THE OUTLET OF A LABORATORY PRECIPITATOR

Radius Size Range	No. Part	Mean Charge	Min Charge	Max Charge	Normalized Standard Deviation	Predicted Charge
(10^{-6}m)		(coul)	(coul)	(coul)		(coul)
0.25-0.35	3	1.28×10^{-17}	4.20×10^{-18}	1.82×10^{-17}	0.481	1.61×10^{-17}
0.35-0.45	35	1.98×10^{-17}	5.22×10^{-18}	3.82×10^{-17}	0.270	2.62×10^{-17}
0.45-0.55	57	2.88×10^{-17}	1.96×10^{-17}	6.03×10^{-17}	0.265	3.81×10^{-17}
0.55-0.65	46	4.54×10^{-17}	2.76×10^{-17}	1.17×10^{-16}	0.346	5.16×10^{-17}
0.65-0.75	68	6.71×10^{-17}	3.74×10^{-17}	1.04×10^{-16}	0.234	6.75×10^{-17}
0.75-0.85	80	9.10×10^{-17}	4.16×10^{-17}	1.58×10^{-16}	0.271	8.49×10^{-17}
0.85-0.95	66	1.21×10^{-16}	6.41×10^{-17}	1.87×10^{-16}	0.280	1.05×10^{-16}
0.95-1.05	56	1.43×10^{-16}	6.08×10^{-17}	2.68×10^{-16}	0.330	1.26×10^{-16}
1.05-1.15	42	1.64×10^{-16}	8.09×10^{-17}	2.94×10^{-16}	0.306	1.48×10^{-16}
1.15-1.25	20	1.82×10^{-16}	1.16×10^{-16}	3.17×10^{-16}	0.289	1.75×10^{-16}
1.25-1.35	5	3.32×10^{-16}	2.39×10^{-16}	4.39×10^{-16}	0.237	2.02×10^{-16}
1.35-1.45	6	2.61×10^{-16}	1.48×10^{-16}	4.93×10^{-16}	0.438	2.31×10^{-16}
1.45-1.55	2	4.30×10^{-16}	3.95×10^{-16}	4.59×10^{-16}	0.748	2.61×10^{-16}

The solid curve is a model[4] prediction of charge as a function of particle radius at the outlet of the precipitator. The model employs an ionic charging theory.[5]

In a wire-plate geometry, the electric field does not vary significantly over a major portion of the interelectrode space and it varies rapidly only over a small high field region near the discharge electrode.[6] Thus, one would expect that the majority of the particles of a given radius exiting the precipitator would have essentially the same charge but there would be a spread in charge lying in a range determined by the minimum and maximum values of the electric field. These expectations are evidenced in the data in that the normalized standard deviations are small. One might also expect that a certain percentage (possibly 5-10%) of the smaller particles (less than 0.5 μm in radius) would pass through high electric field regions near the discharge electrodes and would acquire charges which are significantly higher than those predicted by the average electric field used in the model. Although values of the electric field in the high field region should be up to 8.5 times the average value of electric field used in the model, the ratios of measured charge to predicted charge did not exceed a value of 2.8. It was also observed that, while it was relatively easy to find particle charges significantly larger than that predicted by the model for radii greater than approximately 0.7 μm, very few particles were found to have a significantly higher charge than predicted by the model for radii less than approximately 0.7 μm. In fact, in the range of radius between 0.2 and 0.8 μm, only one particle out of 289 measured had a charge which was over a factor of 1.6 times the predicted charge. In addition many samples were observed in which the particles larger than 0.5 μm in radius were allowed to settle out in order to determine if highly charged submicron particles were present. In all these samples, the remaining particles all moved with essentially the same velocity in an applied electric field. Thus, they all had approximately the same value of charge. Measurements made on gas samples taken from the middle of the inlet electrical section also produced the same results.

The limited data shown in Figure 2 and Table 1 indicate that the measurement technique is reliable and that the model predictions are in good agreement with the average measured value of particle charge. The higher theoretical predictions for particle radii less than 0.6 μm are inherent in the approximate theory at the values of electric field which were utilized in the experiment. The use of an average electric field determined by dividing the applied voltage by the wire-to-plate spacing and of a particle residence time determined by dividing the precipitator length by the average gas velocity appears to be adequate for

predicting particle charge. Also, an ionic charging theory appears to be adequate for describing the data.

The objective of the present experimental program was to make charge and radius measurements in a typical full-scale, electrode geometry under both positive and negative corona at various temperatures up to that which is typical in a hot-side precipitator. In these experiments, the gas stream entering the precipitator was laboratory air containing low resistivity, redispersed fly ash particles. In principle, although sparkover may occur at a different applied voltage for positive corona than negative corona in laboratory air at atmospheric pressure near sea level, the clean air, clean plate, voltage-current curves for the two cases should be nearly the same up to sparkover for typical full-scale plate spacings since the starting voltages and effective ion mobilities do not differ appreciably. Thus, for low mass loadings of low resistivity fly ash particles, comparisons of particle charging capabilities of positive and negative corona might be made where essentially the same applied voltages and currents are utilized in both cases. Any significant differences in particle charging capabilities under these conditions would indicate different charging mechanisms for the different types of corona.

At higher temperatures (and/or reduced pressures), the mean-free-paths of ions and electrons increase. Thus, in the case of negative corona, free electrons can penetrate further into the interelectrode space and possibly can have an increased effect on voltage-current characteristics and particle charging. Comparison of voltage-current characteristics and particle charging for both positive and negative corona at higher temperatures should provide further insight into the effect, if any, of free electrons. If significant penetration of free electrons occurs in the interelectrode space, this might be evidenced in a larger difference in positive and negative voltage-current characteristics than would be obtained if only ions carried the current. However, even if differences in voltage-current characteristics can not be firmly established, differences in particle charging capabilities may still exist.

The effect of temperature on particle charging was examined in laboratory Precipitators B and C. Precipitator B has one gas passage, four electrical sections which are 91.4 cm (36 in.) long, plates which are 91.4 cm (36 in.) high, a 25.4 cm (10 in.) plate-to-plate spacing, a 22.9 cm (9 in.) wire-to-wire spacing, a 0.32 cm (0.125 in.) discharge electrode (wire) diameter. Precipitator C has one gas passage, four electrical sections which are 1.22 m (4 ft) long, plates which are 1.22 m (4 ft) high, a 25.4 cm (10 in.) plate-to-plate spacing, a 22.9 cm (9 in.) wire-to-wire spacing and a 0.32 cm (0.125 in.) discharge electrode (wire) diameter. Measurements at 38°C (100°F) were performed at the outlet of Precipitator B, while measurements at 148°C (300°F),

232°C (450°F), and 343°C (650°F) were performed at the outlet of Precipitator C.

Figures 3-5 show typical real time voltage-current traces obtained from Precipitator C for clean air, wires, and plates at three different temperatures. All these curves were obtained sequentially over a relatively short time period. Under these conditions and with good electrode alignment, it can be seen that voltage-current curves which are nearly coincident are obtainable. Figures 6-8 show some typical average voltage-current curves obtained when the air stream contained fly ash particles and when the wires and plates were somewhat dirty. The data in Figure 6 represent an average over Precipitator B. The data in Figures 7 and 8 were obtained from Precipitator C with curves from all the electrical sections shown in Figure 7 and an average over the entire precipitator shown in Figure 8. All data with particles in the air stream obtained at 343°C (650°F) from Precipitator C were acquired approximately four months prior to that at 148°C (300°F) and 232°C (450°F). During the later measurement period, the precipitator was not operating as well as before, and the voltage-current curves with particles for positive and negative corona were widely separated. Since the inlet mass loading was nominally on the order of 1.14 gm/m^3 (0.5 gr/acf) and the particle size distribution was rather large, the effect of particles on the voltage-current curves could not be attributed entirely to a particulate space charge effect in the gas. The observed behavior of the voltage-current curves might have been due to deposits of a high resistivity ash on the wires and plates acquired during other experiments performed just prior to these measurements. In any event, it was often observed that the addition of particles caused the positive and negative voltage-current curves to separate to a larger extent than anticipated.

Figures 9-11 show particle radius and charge measurements made at the outlet of Precipitator B at 38°C (100°F) with an average gas velocity of approximately 1.5 m/sec (5.0 ft/sec). These and additional data are tabulated in Tables 2-5. Model predictions for the different conditions are also shown for comparison with the data. The data in Figure 9 were obtained with a constant average current density of 15 nA/cm^2 (13.9 $\mu A/ft^2$) and average applied voltages for positive and negative corona of 38.0 kV and 34.5 kV, respectively. The data in Figure 10 were obtained with a constant average applied voltage of 35.0 kV and average current densities for positive and negative corona of 9 nA/cm^2 (8.4 $\mu A/ft^2$) and 15 nA/cm^2 (13.9 $\mu A/ft^2$), respectively. The data in Figure 11 were obtained for negative corona only at average applied voltages of 34.5 kV and 38.0 kV, corresponding to average current densities of 15 nA/cm^2 (13.9 $\mu A/ft^2$) and 36 nA/cm^2 (33.4 $\mu A/ft^2$), respectively. For all the data at 38°C (100°F), the theory and data show good

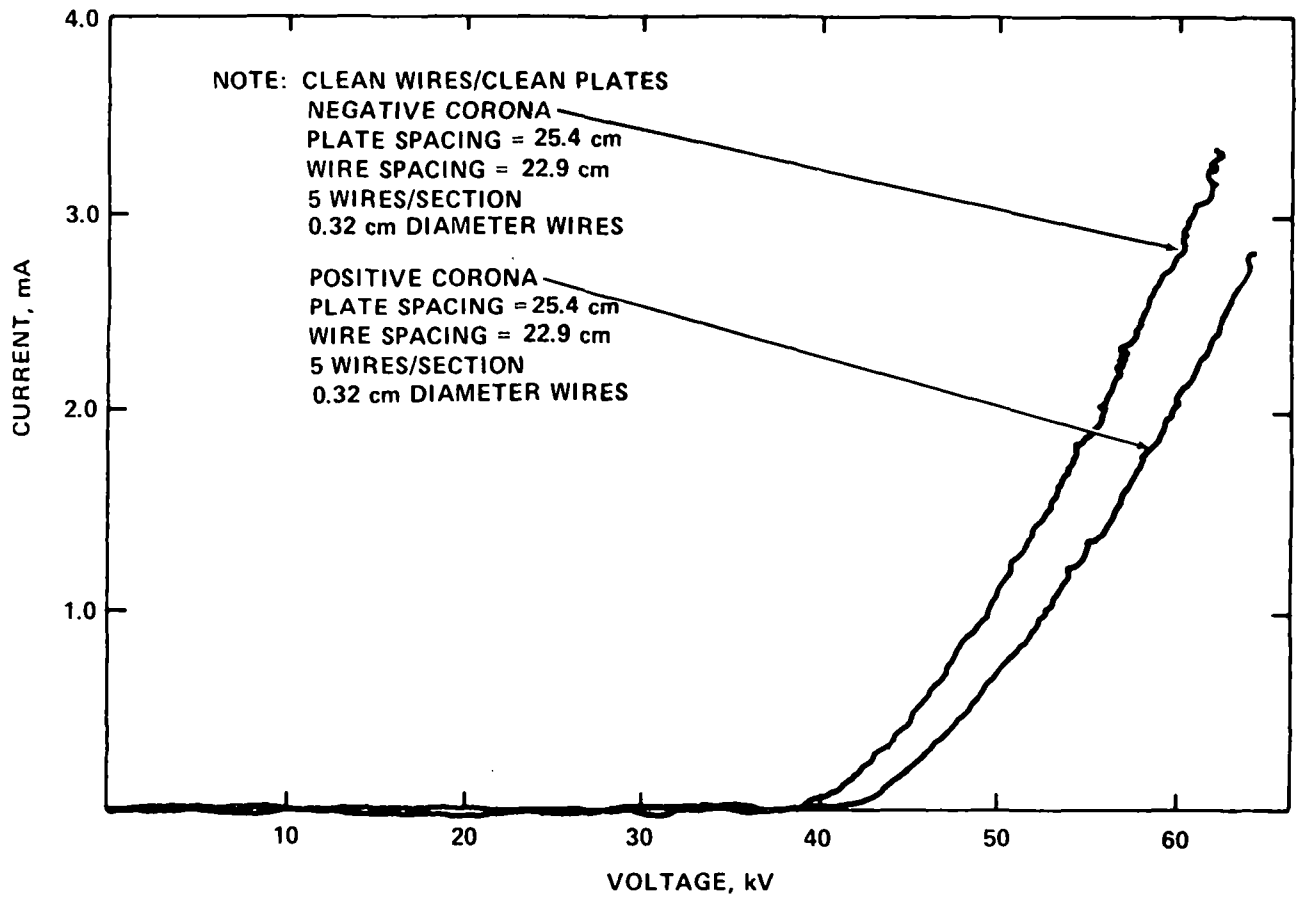

Figure 3. Clean air, wire, and plate voltage-current curves for Precipitator C at ambient temperature.

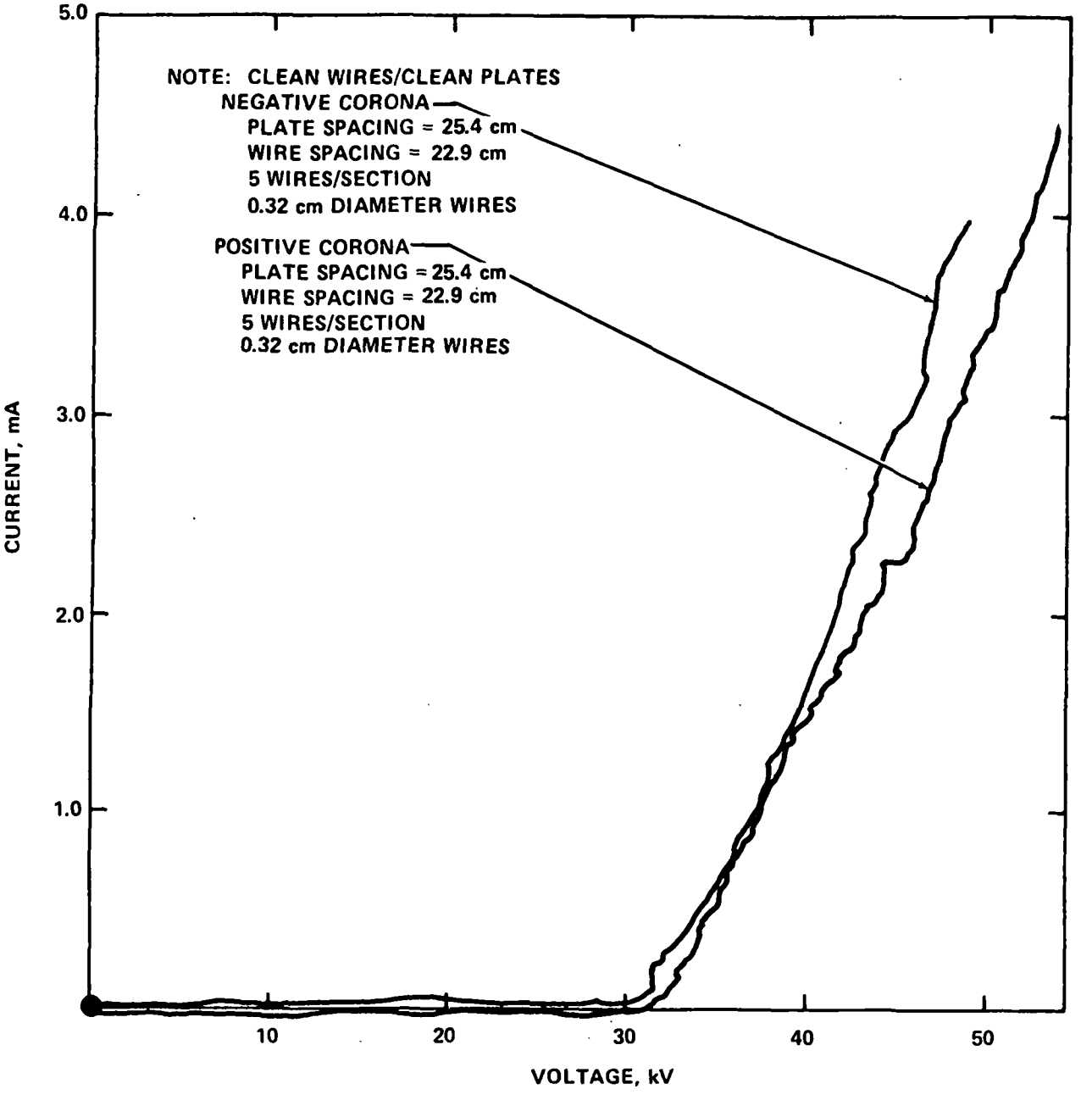

Figure 4. Clean air, wire, and plate voltage-current curves for Precipitator C at 148°C (300°F).

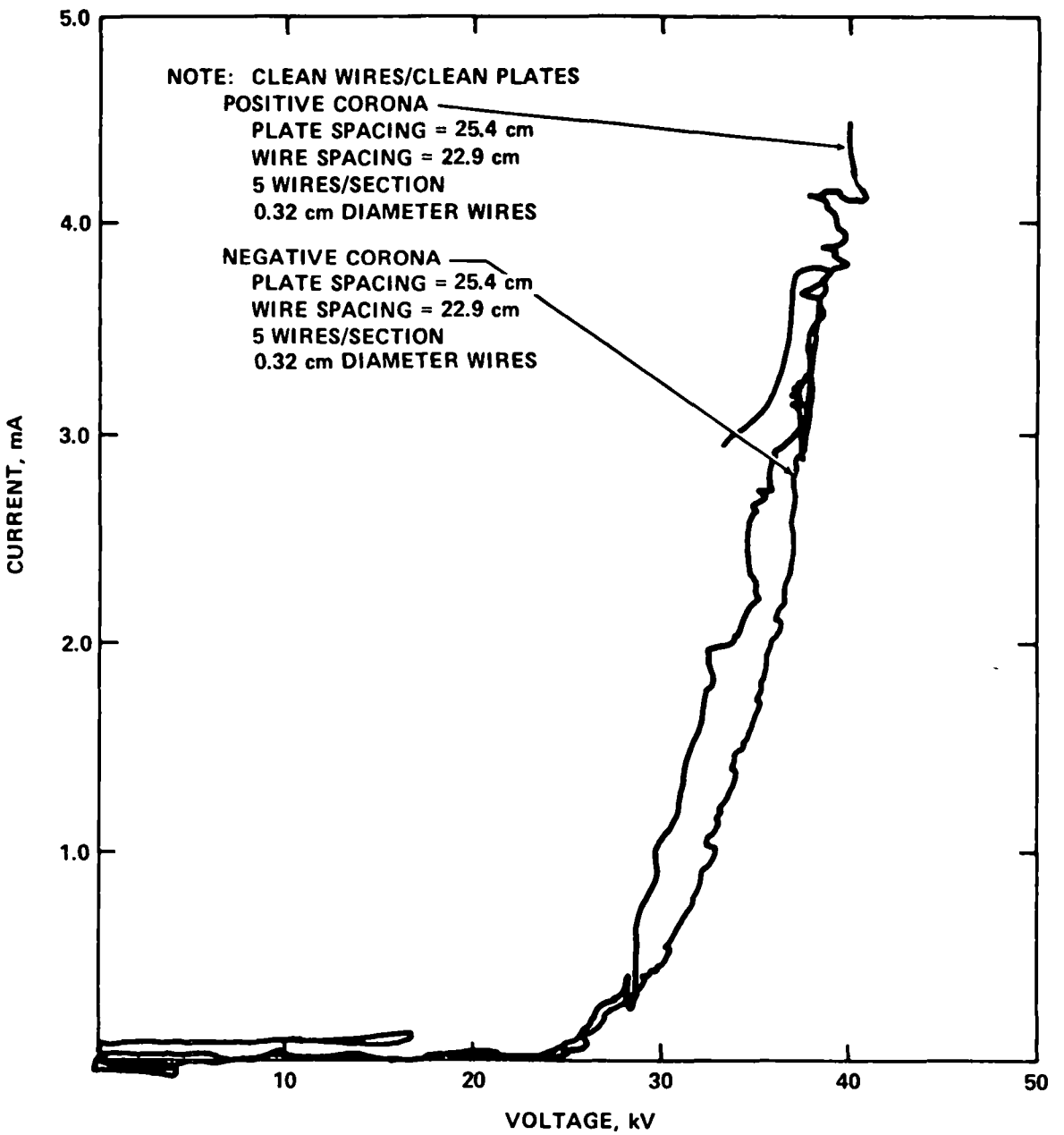

Figure 5. Clean air, wire, and plate voltage-current curves for Precipitator C at 343°C (650°F).

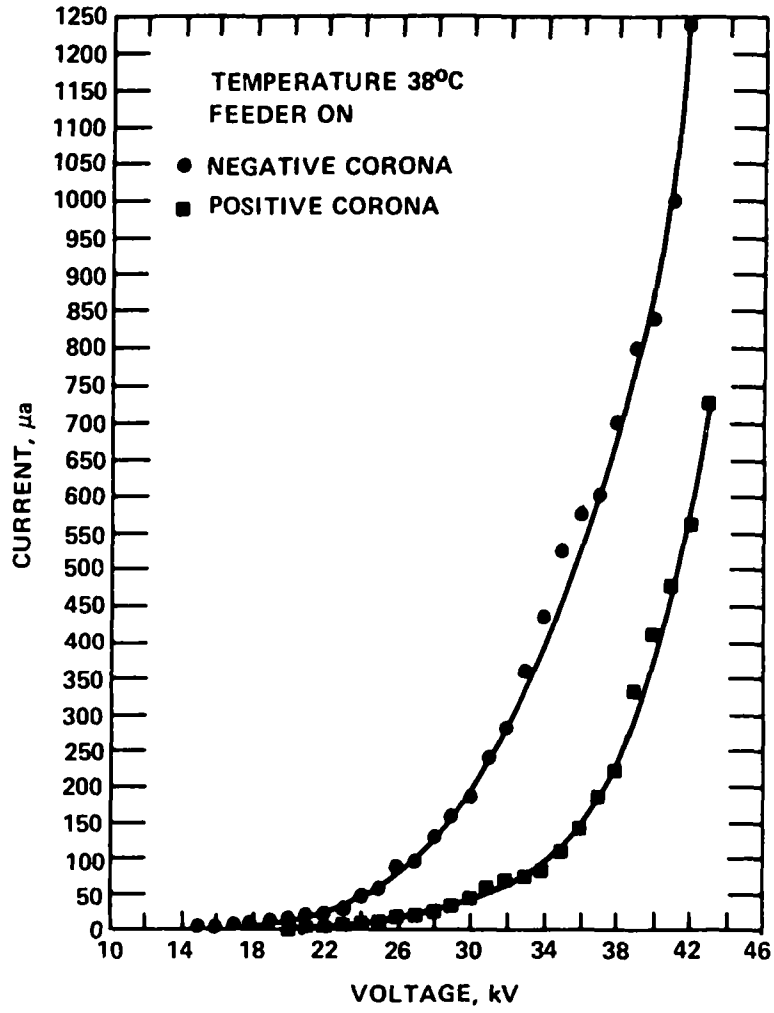

Figure 6. Average voltage-current curves with particles for Precipitator B at 38°C (100°F).

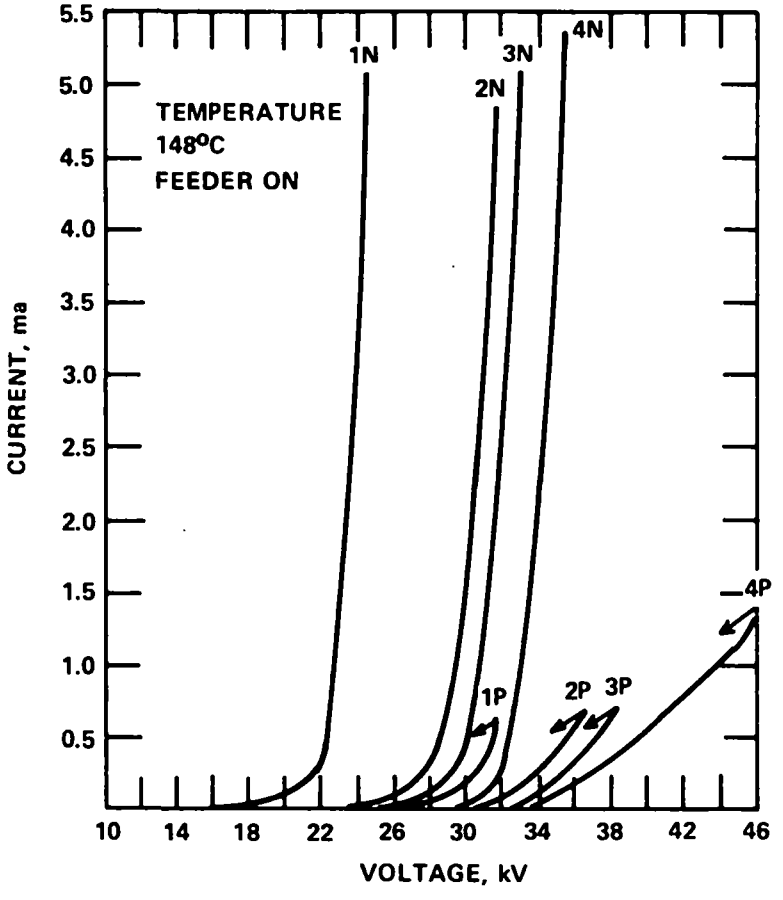

Figure 7. Voltage-current curves for the different electrical sections with particles for Precipitator C at 148°C (300°F).

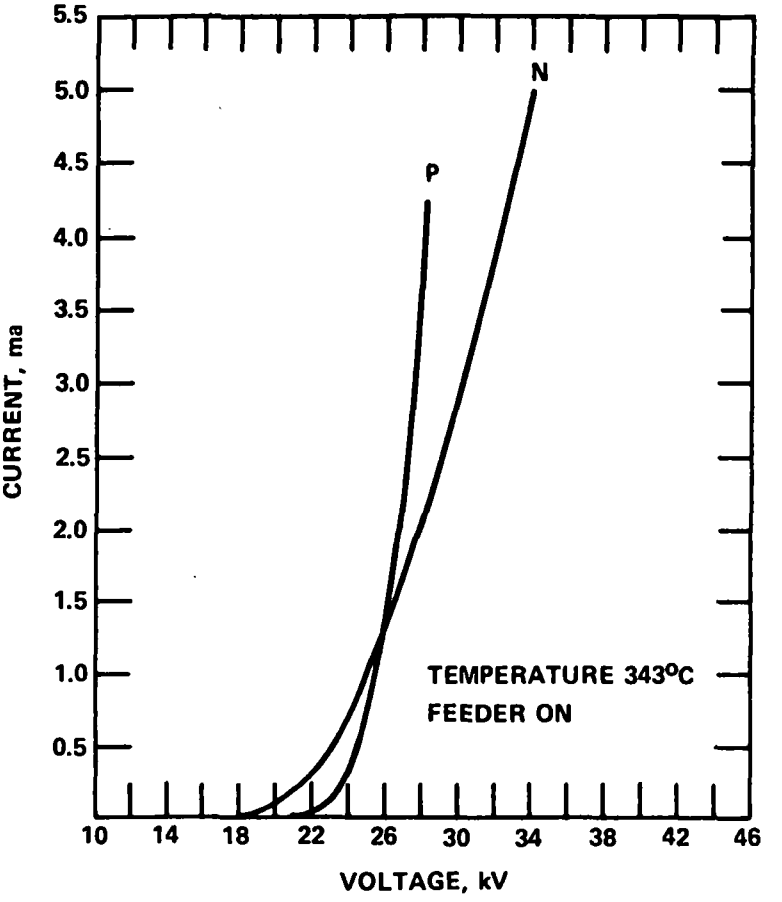

Figure 8. Average voltage-current curves with particles for Precipitator C at 343°C (650°F).

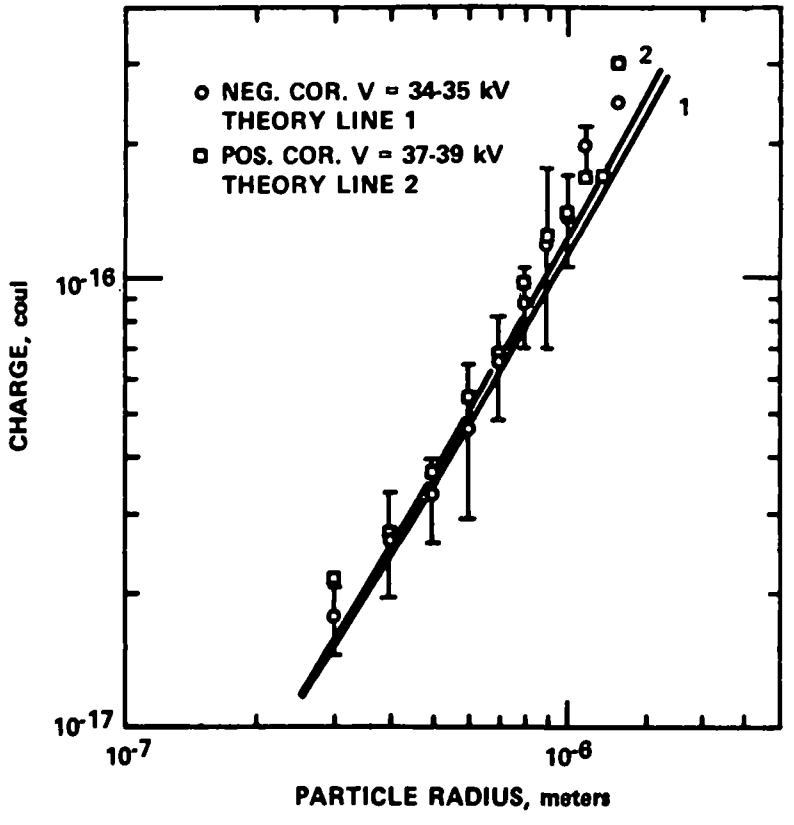

Figure 9. Measured positive and negative particle charge versus measured radius and comparison with theory at 38°C (100°F) and 15 nA/cm^2 (13.9 μA/ft^2).

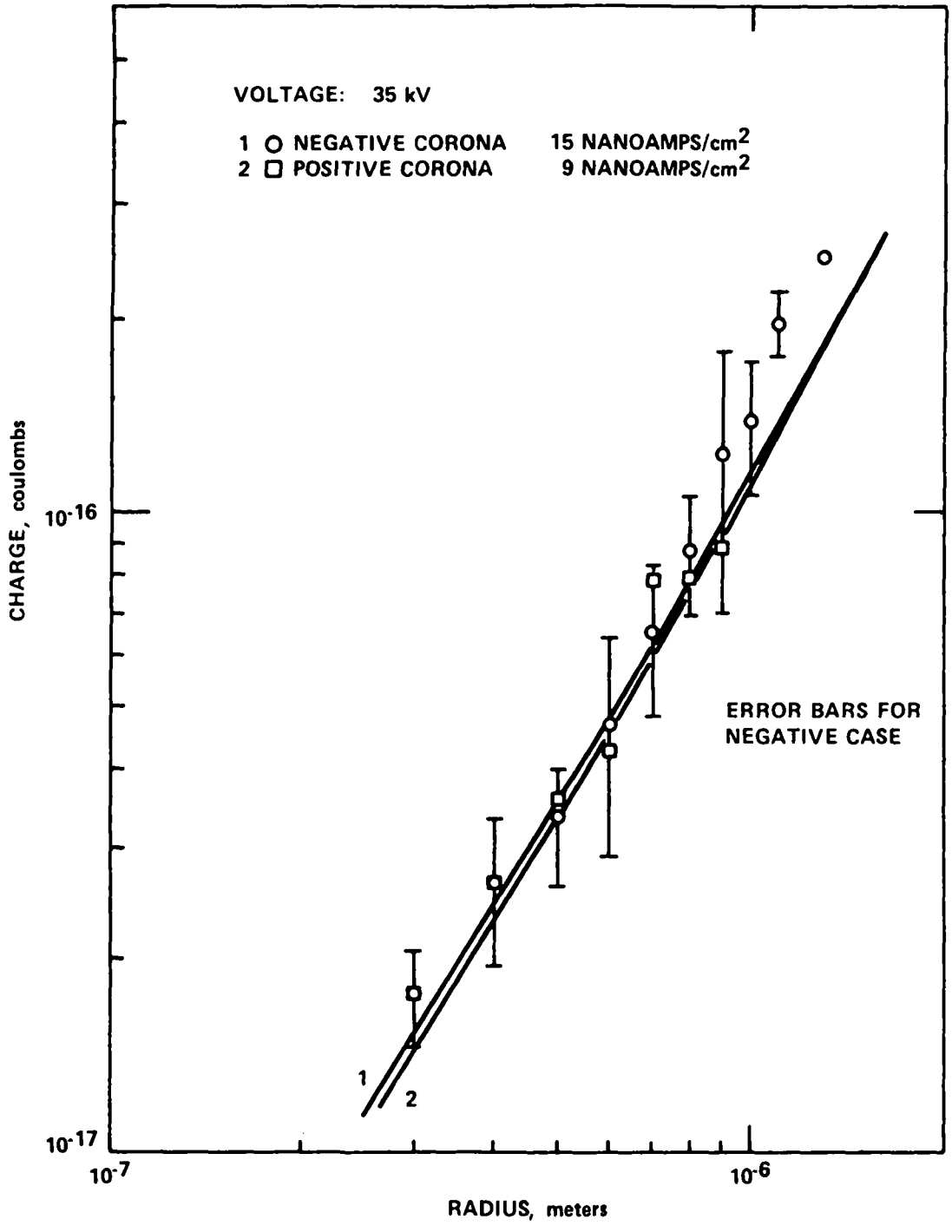

Figure 10. Measured positive and negative particle charge versus measured radius and comparison with theory at 38°C (100°F) and 35 kV.

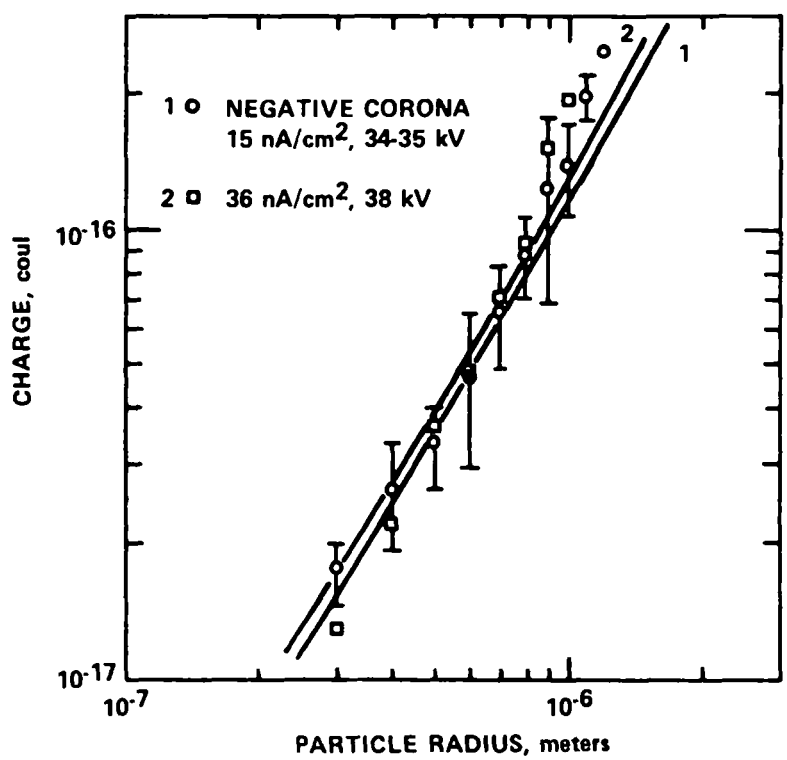

Figure 11. Measured negative particle charge versus measured radius and comparison with theory at 38°C (100°F) with 15 nA/cm^2 (13.9 μA/ft^2) and 36 nA/cm^2 (33.4 μA/ft^2).

TABLE 2

PARTICLE CHARGE FOR POSITIVE CORONA
AT 38°C, 37-39 kV, 15 nA/cm^2

Median Radius of Size Band (microns)	Number of Particles in Size Band	Average Charge/ Particle (10^{-17} coulombs)	Standard Deviation (10^{-17} coulombs)	Normalized Standard Deviation	Average Number of Charges/ Particle
0.3	15	2.155	0.7507	0.35	135
0.4	23	2.733	0.8730	0.32	171
0.5	23	3.705	0.8348	0.23	232
0.6	28	5.419	1.750	0.32	339
0.7	14	6.777	1.692	0.25	424
0.8	16	9.745	3.122	0.32	609
0.9	7	12.00	4.430	0.37	750
1.0	7	13.71	1.423	0.10	857
1.1	5	16.91	2.786	0.16	1057
1.2	1	16.85	---	---	1053
1.3	2	30.56	2.295	0.08	1910

TABLE 3

PARTICLE CHARGE FOR NEGATIVE CORONA
AT 38°C, 34-35 kV, 15 nA/cm^2

Median Radius of Size Band (microns)	Number of Particles in Size Band	Average Charge/ Particle (10^{-17} coulombs)	Standard Deviation (10^{-17} coulombs)	Normalized Standard Deviation	Average Number of Charges/ Particle
0.3	2	1.777	0.3136	0.18	111
0.4	15	2.644	0.7142	0.27	165
0.5	39	3.314	0.6943	0.21	207
0.6	25	4.662	1.755	0.38	291
0.7	31	6.551	1.758	0.27	409
0.8	17	8.765	1.888	0.22	548
0.9	12	12.28	5.462	0.44	768
1.0	3	13.85	3.261	0.24	866
1.1	3	19.62	2.307	0.12	1226
1.2	---	---	---	---	---
1.3	1	24.78	---	---	1549

TABLE 4

PARTICLE CHARGE FOR POSITIVE CORONA
AT 38°C, 35 kV, 9 nA/cm^2

Median Radius of Size Band (microns)	Number of Particles in Size Band	Average Charge/ Particle (10^{-17} coulombs)	Standard Deviation (10^{-17} coulombs)	Normalized Standard Deviation	Average Number of Charges/ Particle
0.3	34	1.761	0.5945	0.34	110
0.4	16	2.639	0.8297	0.31	165
0.5	15	3.556	1.116	0.31	222
0.6	19	4.268	1.018	0.24	267
0.7	10	7.860	3.071	0.39	491
0.8	4	7.926	0.5088	0.06	495
0.9	3	8.799	1.056	0.12	550

TABLE 5

PARTICLE CHARGE FOR NEGATIVE CORONA
AT 38°C, 38 kV, 36 nA/cm^2

Median Radius of Size Band (microns)	Number of Particles in Size Band	Average Charge/ Particle (10^{-17} coulombs)	Standard Deviation (10^{-17} coulombs)	Normalized Standard Deviation	Average Number of Charges/ Particle
0.3	20	1.278	0.3608	0.28	80
0.4	32	2.219	0.5699	0.26	139
0.5	38	3.623	1.048	0.29	226
0.6	28	4.808	1.125	0.23	301
0.7	17	7.110	2.450	0.34	444
0.8	9	9.251	2.890	0.31	578
0.9	4	15.25	4.337	0.28	953
1.0	3	14.30	1.345	0.09	894

agreement. Since the least amount of data was acquired for the smallest and largest radius bands, the agreement with theory should be expected to be less for these particle radii.

Figure 12 shows particle radius and charge measurements made at the outlet of Precipitator C at 148°C (300°F) with an average gas velocity of approximately 1.4 m/sec (4.5 ft/sec). These and additional data are tabulated in Tables 6 and 7. The average applied voltage and current density for negative corona were 25.7 kV and 31.0 nA/cm^2 (28.8 μA/ft^2), respectively. The average applied voltage and current density for positive corona were 33.0 kV and 18.0 nA/cm^2 (16.7 μA/ft^2), respectively. During measurements with both positive and negative corona, it was difficult to maintain constant electrical operating conditions. Wide fluctuations in applied voltage and current occurred with intermittent sparking. Thus, these data are not useful for comparing positive and negative particle charging under comparable conditions. However, the data give an illustration of the capability of the measurement system to detect adverse charging conditions.

Figure 13 shows particle radius and charge measurements made at the outlet of Precipitator C at 232°C (450°F) with an average gas velocity of approximately 1.4 m/sec (4.5 ft/sec). These and additional data are tabulated in Tables 8 and 9. The average applied voltage and current density for negative corona were 28.1 kV and 28.0 nA/cm^2 (26.0 μA/ft^2), respectively. The average applied voltage and current density for positive corona were 31.5 kV and 17 nA/cm^2 (15.8 μA/ft^2), respectively. After the measurements at 148°C (300°F), the wires and plates of the precipitator were cleaned by brushing. This resulted in more favorable and stable electrical operating conditions. For the operating conditions during the measurements, the theory predicts essentially the same charge versus radius relationship for the positive and negative corona conditions. While the theory agrees well with the data obtained with positive corona for all particle radii, it clearly underpredicts negative particle charge for radii between approximately 0.7 μm and 1.2 μm. In this range of radius, the ratio of the average measured negative charge to the predicted charge varies from 1.25 to 1.59, increasing with increasing diameter. These data indicate that negative corona is more effective than positive corona in charging particles with radii between 0.7 μm and 1.2 μm at 232°C (450°F). Comparison of these data with the theoretical predictions and the information in Figures 2-5 suggests that the use of a completely ionic charging theory to describe negative particle charging at 232°C (450°F) is inadequate. Since the only major physical difference between the positive and negative corona process is the free electron penetration into the interelectrode space in the negative corona case, the enhanced particle charge with negative corona at 232°C (450°F) might be due to increased free electron charging.

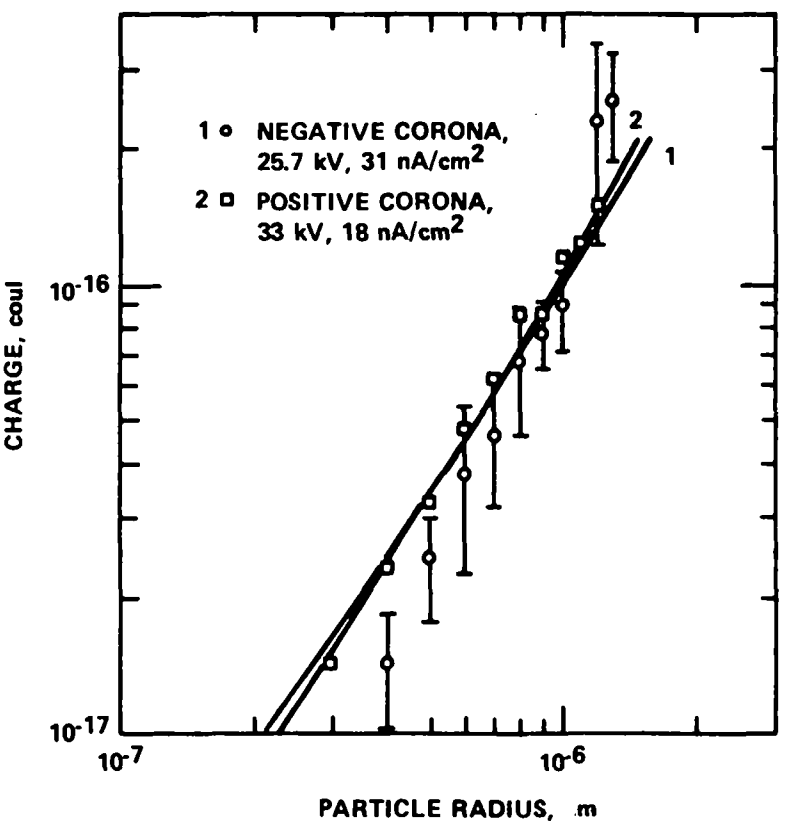

Figure 12. Measured positive and negative particle charge versus measured radius and comparison with theory at 148°C (300°F).

TABLE 6

PARTICLE CHARGE FOR POSITIVE CORONA
AT 148°C, 33.0 kV, 18 nA/cm^2

Median Radius of Size Band (microns)	Number of Particles in Size Band	Average Charge/ Particle (10^{-17} coulombs)	Standard Deviation (10^{-17} coulombs)	Normalized Standard Deviation	Average Number of Charges/ Particle
0.3	5	1.428	0.1032	0.081	89
0.4	15	2.342	0.5156	0.2202	146
0.5	19	3.243	0.8471	0.2612	203
0.6	18	4.743	0.8260	0.1741	296
0.7	27	6.115	1.840	0.3009	382
0.8	19	8.470	1.994	0.2354	529
0.9	23	8.498	2.058	0.2421	531
1.0	13	11.31	3.769	0.3333	707
1.1	6	12.32	0.6139	0.0498	770
1.2	6	15.02	1.938	0.1291	939

TABLE 7

PARTICLE CHARGE FOR NEGATIVE CORONA
AT 148°C, 25.7 kV, 31 nA/cm^2

Median Radius of Size Band (microns)	Number of Particles in Size Band	Average Charge/ Particle (10^{-17} coulombs)	Standard Deviation (10^{-17} coulombs)	Normalized Standard Deviation	Average Number of Charges/ Particle
0.4	14	1.447	0.6014	0.4156	90
0.5	28	2.426	0.6695	0.2759	152
0.6	36	3.799	1.544	0.4064	237
0.7	30	4.627	1.513	0.3270	289
0.8	10	6.710	2.195	0.3271	419
0.9	16	7.773	1.381	0.1777	486
1.0	7	8.862	1.827	0.2061	554
1.2	3	23.09	11.043	0.4516	1443
1.3	4	25.62	7.145	0.2788	1601

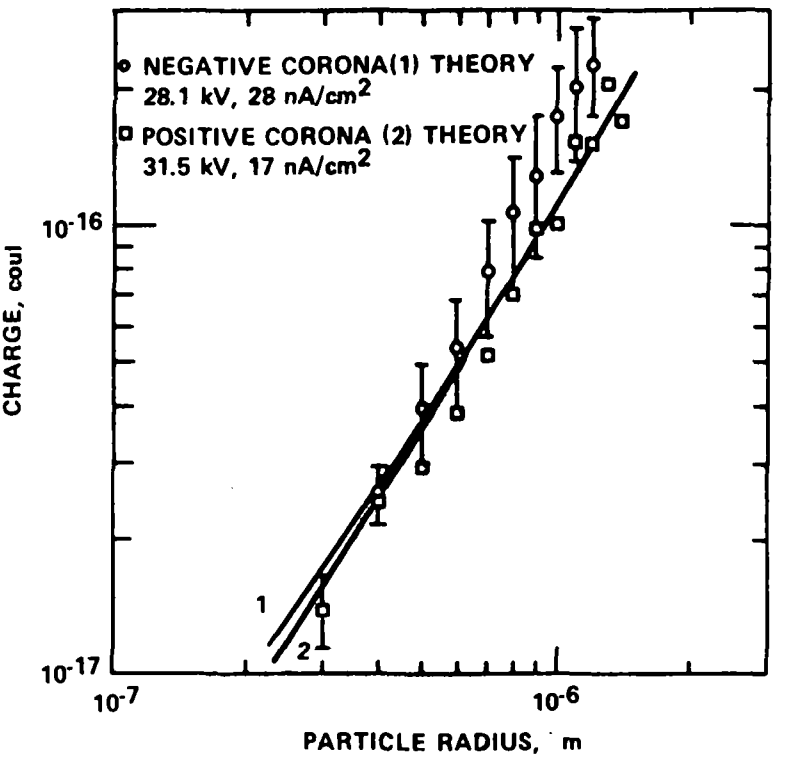

Figure 13. Measured positive and negative particle charge versus measured radius and comparison with theory at 232°C (450°F).

TABLE 8

PARTICLE CHARGE FOR POSITIVE CORONA
AT 232°C, 31.5 kV, 17 nA/cm^2

Median Radius of Size Band (microns)	Number of Particles in Size Band	Average Charge/ Particle (10^{-17} coulombs)	Standard Deviation (10^{-17} coulombs)	Normalized Standard Deviation	Average Number of Charges/ Particle
0.3	9	1.405	0.2762	0.1966	88
0.4	10	2.461	0.5891	0.2393	154
0.5	19	2.938	0.8750	0.2978	183
0.6	29	3.886	0.9217	0.2372	243
0.7	17	5.201	1.118	0.2150	325
0.8	23	7.027	2.891	0.4114	439
0.9	17	9.857	3.555	0.3607	616
1.0	13	9.925	2.020	0.2036	620
1.1	4	15.36	4.012	0.2612	960
1.3	2	20.78	6.675	0.3213	1299
1.4	2	17.00	8.368	0.4922	1063

TABLE 9

PARTICLE CHARGE FOR NEGATIVE CORONA
AT 232°C, 28.1 kV, 28 nA/cm^2

Median Radius of Size Band (microns)	Number of Particles in Size Band	Average Charge/ Particle (10^{-17} coulombs)	Standard Deviation (10^{-17} coulombs)	Normalized Standard Deviation	Average Number of Charges/ Particle
0.4	5	2.568	0.3808	0.1483	161
0.5	32	3.959	0.9971	0.2518	247
0.6	32	5.413	1.470	0.2715	338
0.7	24	7.989	2.372	0.2967	499
0.8	21	10.62	3.506	0.3303	664
0.9	14	12.85	4.321	0.3362	803
1.0	4	17.64	4.570	0.2591	1102
1.1	9	20.57	6.723	0.3268	1286
1.2	5	22.89	5.570	0.2434	1431
1.3	3	20.88	4.038	0.1934	1305

Figures 14-16 show particle radius and charge measurements made at the outlet of Precipitator C at 343°C (650°F) with an average gas velocity of approximately 1.4 m/sec (4.5 ft/sec). These and additional data are tabulated in Tables 10-13. The precipitator had been cleaned thoroughly prior to these measurements. During the measurements, the electrical operating conditions were extremely stable. The data shown in Figure 14 were obtained for a current density of 30 nA/cm^2 (27.9 μA/ft) for both positive and negative corona with essentially the same average applied voltages of 26.5 kV and 27.5 kV, respectively. Similar to the results obtained at 232°C (450°F), the theory agrees reasonably well with the data for positive corona but clearly underpredicts particle charge obtained with negative corona for radii between approximately 0.6 μm and 1.3 μm. In this range of radius, the ratio of the average measured negative charge to the predicted charge ranges from 1.27 to 1.94, generally increasing with increasing diameter. These data again suggest the possibility of free electrons participating in the charging process with negative corona.

Figures 15 and 16 contain data showing the effect of electrical conditions on particle charging with positive and negative corona at 343°C (650°F). Again, the theory agrees relatively well with the data for positive corona but underpredicts particle charge obtained with negative corona for radii between approximately 0.6 μm and 1.3 μm. The data show the same trend as the theory in that larger applied voltages and current densities result in higher values of particle charge. Also, the ability for negative corona to acquire a significantly higher voltage and current density prior to sparkover resulted in a further increase in particle charge as compared to the positive corona.

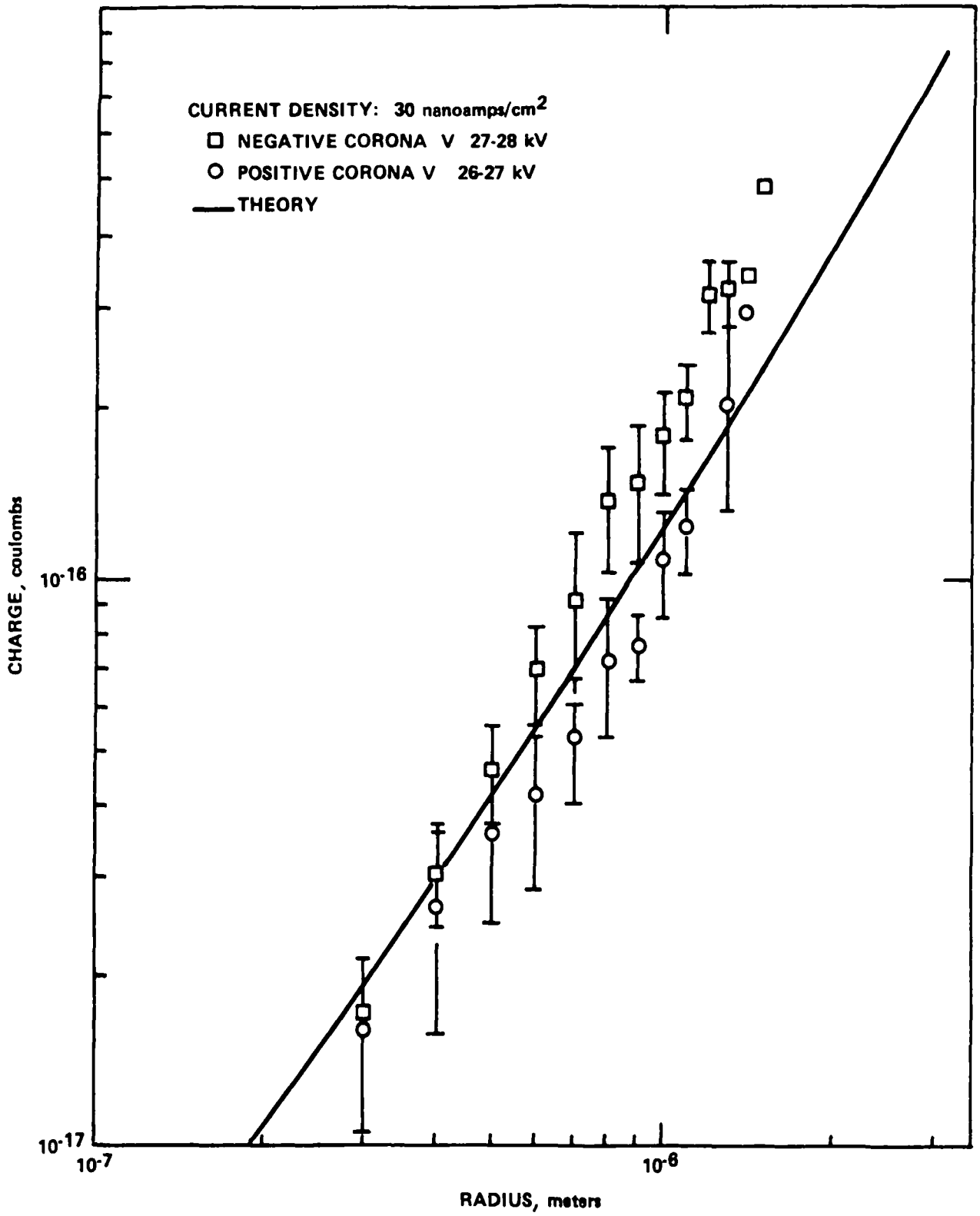

Figure 14. Measured positive and negative particle charge versus measured radius and comparison with theory at 343°C (650°F) and 30 nA/cm^2 (27.9 μA/ft^2).

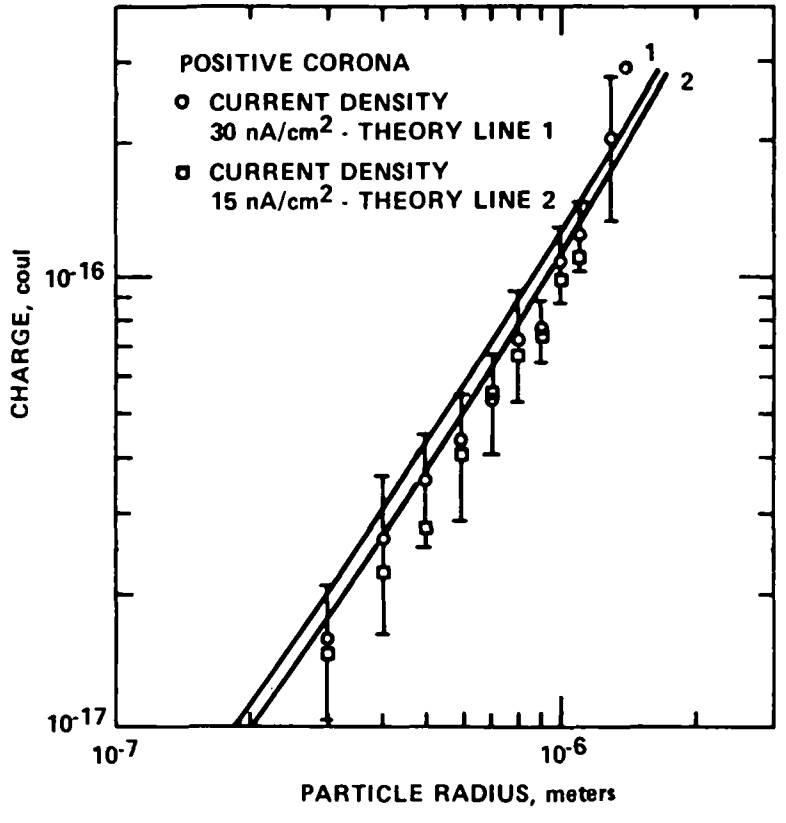

Figure 15. Measured positive particle charge versus measured radius and comparison with theory at 343°C (650°F) with 15 nA/cm^2 (13.9 μA/ft^2) and 30 nA/cm^2 (27.9 μA/ft^2).

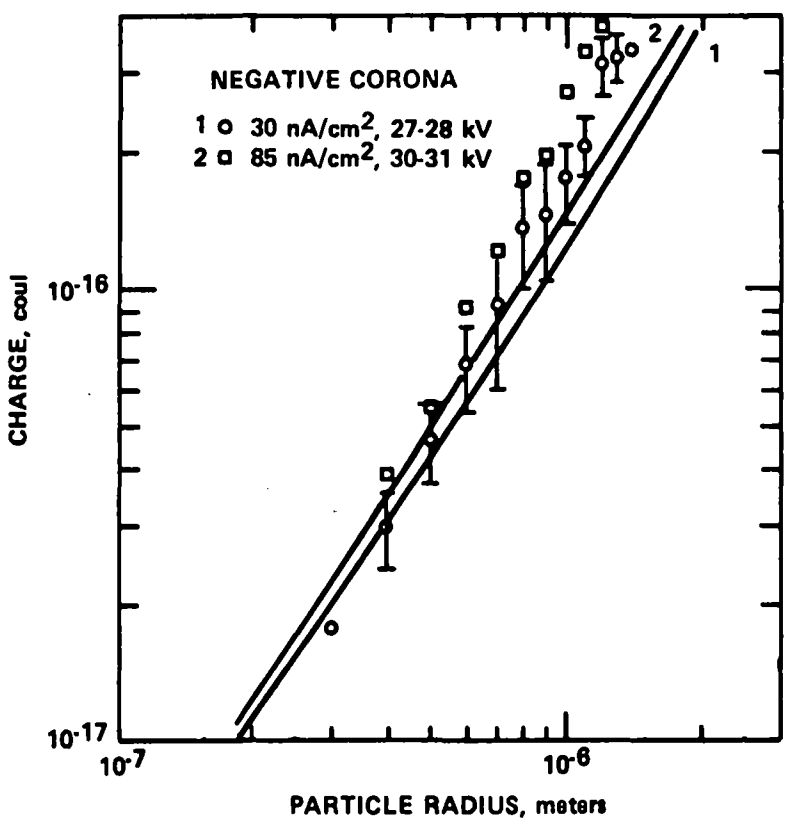

Figure 16. Measured negative particle charge versus measured radius and comparison with theory at 343°C (650°F) with 30 nA/cm^2 (27.9 μA/ft^2) and 85 nA/cm^2 (79.0 μA/ft^2).

TABLE 10

PARTICLE CHARGE FOR POSITIVE CORONA
AT 343°C, 26-27 kV, 30 nA/cm^2

Median Radius of Size Band (microns)	Number of Particles in Size Band	Average Charge/ Particle (10^{-17} coulombs)	Standard Deviation (10^{-17} coulombs)	Normalized Standard Deviation	Average Number of Charges/ Particle
0.3	9	1.598	0.5438	0.34	99
0.4	16	2.642	1.083	0.41	165
0.5	21	3.582	1.094	0.31	224
0.6	19	4.186	1.349	0.32	262
0.7	28	5.385	1.342	0.25	337
0.8	9	7.255	2.037	0.28	453
0.9	14	7.613	1.130	0.15	476
1.0	12	10.91	2.364	0.22	682
1.1	7	12.30	2.212	0.18	769
1.2	1	25.20	---	---	1575
1.3	7	20.42	7.253	0.35	1276
1.4	1	29.38	---	---	1836

TABLE 11

PARTICLE CHARGE FOR NEGATIVE CORONA
AT 343°C, 27-28 kV, 30 nA/cm^2

Median Radius of Size Band (microns)	Number of Particles in Size Band	Average Charge/ Particle (10^{-17} coulombs)	Standard Deviation (10^{-17} coulombs)	Normalized Standard Deviation	Average Number of Charges/ Particle
0.3	1	1.717	---	---	107
0.4	6	3.004	0.5930	0.20	188
0.5	19	4.640	0.9379	0.20	290
0.6	27	6.836	1.550	0.23	427
0.7	32	9.193	3.131	0.34	575
0.8	16	13.69	3.570	0.26	856
0.9	17	14.60	4.116	0.28	913
1.0	12	17.60	3.632	0.21	1100
1.1	7	20.76	3.274	0.16	1298
1.2	5	31.46	4.783	0.15	1966
1.3	4	32.16	4.225	0.13	2006
1.4	2	33.71	0.085	0.002	2107
1.5	1	48.38	---	---	3024

TABLE 12

PARTICLE CHARGE FOR POSITIVE CORONA
AT 343°C, 25 kV, 15 nA/cm^2

Median Radius of Size Band (microns)	Number of Particles in Size Band	Average Charge/ Particle (10^{-17} coulombs)	Standard Deviation (10^{-17} coulombs)	Normalized Standard Deviation	Average Number of Charges/ Particle
0.3	4	1.463	0.3552	0.24	91
0.4	4	2.235	0.5683	0.25	140
0.5	9	2.787	0.7414	0.27	174
0.6	6	4.018	0.6848	0.17	251
0.7	10	5.572	1.213	0.22	348
0.8	4	6.610	0.9339	0.14	413
0.9	3	7.465	0.7264	0.10	467
1.0	3	9.768	0.0576	0.006	611
1.1	3	11.09	1.097	0.10	693

TABLE 13

PARTICLE CHARGE FOR NEGATIVE CORONA
AT 343°C, 30-31 kV, 85 nA/cm^2

Median Radius of Size Band (microns)	Number of Particles in Size Band	Average Charge/ Particle (10^{-17} coulombs)	Standard Deviation (10^{-17} coulombs)	Normalized Standard Deviation	Average Number of Charges/ Particle
0.3	---	---	---	---	---
0.4	1	3.943	---	---	246
0.5	12	5.533	0.7909	0.14	346
0.6	20	9.137	1.578	0.17	571
0.7	36	12.04	2.256	0.19	753
0.8	26	17.62	3.212	0.18	1101
0.9	27	19.84	3.590	0.18	1240
1.0	11	27.18	4.022	0.15	1699
1.1	7	33.08	5.761	0.17	2068
1.2	2	37.75	1.810	0.05	2359
1.3	2	49.71	7.622	0.15	3107
1.4	2	47.94	7.660	0.16	2996
1.5	1	53.41	---	---	3338

SECTION 6

REFERENCES

1. Penney, G. W., and R. D. Lynch. Measurements of Charge Imparted to Fine Particles by a Corona Discharge. AIEE, 76: 294-299 (July, 1957).

2. Pontius, D. H., L. G. Felix, J. R. McDonald, and W. B. Smith. Fine Particle Charging Development. EPA-600/2-77-173, NTIS PB271-727/AS, U.S. Environmental Protection Agency, Research Triangle Park, North Carolina (1977).

3. Marchant, G. H., Jr., and J. P. Gooch. Performance and Economic Evaluation of a Hot-Side Electrostatic Precipitator. EPA-600/7-78-214, U.S. Environmental Protection Agency, Research Triangle Park, North Carolina (1978).

4. McDonald, J. R. A Mathematical Model of Electrostatic Precipitation (Revision 1): Volume 1. Modeling and Programming. EPA-600/7-78-111a, NTIS PB284-614, U.S. Environmental Protection Agency, Research Triangle Park, North Carolina (1978).

5. Smith, W. B., and J. R. McDonald. Development of a Theory for the Charging of Particles by Unipolar Ions. J. Aerosol Sci., 7:151-166 (1976).

6. McDonald, J. R., W. B. Smith, H. W. Spencer, and L. E. Sparks. A Mathematical Model for Calculating Electrical Conditions in Wire-Duct Electrostatic Precipitation Devices. J. Appl. Phys., 48(6):2231-2246 (1977).

TECHNICAL REPORT DATA
(Please read Instructions on the reverse before completing)

1. REPORT NO.	2.	3. RECIPIENT'S ACCESSION NO.
EPA-600/7-80-077		

4. TITLE AND SUBTITLE	5. REPORT DATE
Charge Measurements of Particles Exiting Electrostatic Precipitators	April 1980
	6. PERFORMING ORGANIZATION CODE
7. AUTHOR(S)	8. PERFORMING ORGANIZATION REPORT NO.
J. R. McDonald, M. H. Anderson, and R. B. Mosley	3858-10 SORI-EAS-80-332
9. PERFORMING ORGANIZATION NAME AND ADDRESS	10. PROGRAM ELEMENT NO.
Southern Research Institute 2000 Ninth Avenue, South Birmingham, Alabama 35205	EHE624
	11. CONTRACT/GRANT NO.
	68-02-2610
12. SPONSORING AGENCY NAME AND ADDRESS	13. TYPE OF REPORT AND PERIOD COVERED
EPA, Office of Research and Development Industrial Environmental Research Laboratory Research Triangle Park, NC 27711	Final; 10/78-10/79
	14. SPONSORING AGENCY CODE
	EPA/600/13

15. SUPPLEMENTARY NOTES IERL-RTP project officer is Leslie E. Sparks, Mail Drop 61, 919/541-2925.

16. ABSTRACT The report gives results of an investigation of particle charging in positive and negative corona discharge as a function of temperature from 38 to 343 C in order to establish, especially at hot-side electrostatic precipitator (ESP) temperatures, the relative effectiveness of the two possible methods of charging. Charge values on individual particles exiting two laboratory ESPs were measured in an experimental apparatus utilizing a Millikan cell. Measurements were directed at fine particles with radii between 0.3 and 1.5 micrometers. Measurements were obtained for redispersed fly ash particles carried in air at temperatures from 38 to 343 C. The electrode geometries and electrical operating conditions utilized were typical of full-scale ESPs. At comparable voltages and currents for positive and negative corona discharges, the ratio of the values of negative to positive charge for radii between 0.6 and 1.3 micrometers were shown to increase from about 1 to 2 as temperatures increased from 37 to 343 C. Predictions of a mathematical model of ESP, employing an ionic charging theory, showed good agreement with all positive charging data; but good agreement was shown with negative charging data only at temperatures below 37 C. Differences between measurements and model predictions are consistent with the postulation of free electron charging at high temperature (negative corona).

17. KEY WORDS AND DOCUMENT ANALYSIS

a. DESCRIPTORS	b. IDENTIFIERS/OPEN ENDED TERMS	c. COSATI Field/Group
Pollution	Pollution Control	13B
Electric Corona	Stationary Sources	13I
Electrostatic Precipitators	Particulate	21B
Fly Ash		11G
Temperature		20C
Dust		14B
Electrical Charge Measurement		

18. DISTRIBUTION STATEMENT	19. SECURITY CLASS *(This Report)*	21. NO. OF PAGES
Release to Public	Unclassified	57
	20. SECURITY CLASS *(This page)* Unclassified	22. PRICE

EPA Form 2220-1 (9-73)